Charge transfer in first layer enhanced Raman scattering and surface resistance

Author:

Andreas Otto

Affiliation:

Institut für experimentelle Physik der kondensierten Materie

Heinrich-Heine-Universität Düsseldorf

Correspondence address:

andreasotto314@gmail.com

Abstract

This article is a revue of surface enhanced Raman scattering (SERS) of molecules adsorbed on roughened silver electrodes and on well-characterized, clean Ag-surfaces in ultra high vacuum (UHV). The resonances of the SERS intensities of pyridine, pyrazine and CN^- adsorbed on roughened silver electrodes shift when using different Laser wavelengths. SERS is quenched by pulling the electrodes out of the electrolyte, thus exposing them to oxygen. The resonances are assigned to transient electron transfer within surface complexes, which arise from roughening silver electrodes. For pyridine and pyrazine an electron is transferred from the Fermi level E_F of the silver electrode to the lowest unoccupied orbital (LUMO). In the case of CN^- the electron is transiently transferred from the highest occupied orbital (HOMO) to E_F. The energy difference between E_F and the LUMO's of pyridine and pyrazine has been measured by inverse photoemission, in good agreement with the results of SERS. The distance dependence of SERS at well-characterized surface s in UHV shows an enhancement of about 100 restricted to the first adsorbed monolayer, on top of the long range electromagnetic (EM) enhancement. Electron energy loss spectroscopy (EELS) of pyrazine and pyridine on Ag(111) has detected weak structures assigned to electron transfer. Charge transfer reactions induce surface resistance.

Introduction

The first proposed explanation of SERS caused by EM enhancement at a rough surface of a noble metal was given by Moskovitz in 1978[1] and at metal spheres by Creighton[2]. One year later Burstein et al.[3] introduced a model based on electron transfer from the metal to the adsorbed molecules. The results of the first 4 years of SERS research since the detection by Fleischmann, Hendra and McQuillan[4], Van Duyne and Jeanmaire[5] and Albrecht and Creighton[6] have been collected in the book edited by Chang and Furtak[7]. Chemical origins of SERS have been described by Furtak et al [8] in 1980. Raman scattering of adsorbates on roughened silver electrodes presents clear evidence for transient electron transfer in Ag- pyridine and to Ag – CN^- complexes[8]. Experiments and results in ultra high vacuum (UHV) obtained by Raman spectroscopy, inverse photoemission and electron energy electron energy loss spectroscopy (EELS) indicate an extra first layer enhancement of about 100 for CO and pyridine physisorbed on Ag(111) surfaces.

Charge transfer excitations in complexes at roughened electrodes

In the sowing article of Jeanmaire and VanDuyne[5], SERS was detected for pyridine adsorbed on silver electrodes roughened (or activated or anodized) by an oxidation-reduction cycle. VanDuyne used only one laser wavelength at 514.5nm., see figure 1.

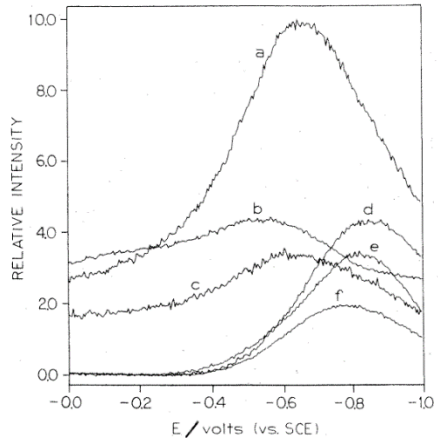

Figure 1) Relative Raman intensity of pyridine adsorbed on a silver electrode as a function of electrode potential E. (a) 1006 cm^{-1}, (b) 1035 cm^{-1}, (c) 3056 cm^{-1}, (d) 1215 cm^{-1}, (e) 1594 cm^{-1}, (f) 623 cm^{-1}. The electrode surface was anodized (roughened) under standard conditions. A relatively large spectrometer band pass (20 cm^{-1}) was used to minimize the error in intensity measurement due to the effect of band frequency changes with electrode potential. Laser excitation wavelength = 514.5 nm. The electrode potential was scanned at a rate of 1.024 Vs^{-1} beginning at 0.0V vs. standard calomel electrode SCE. Each curve was signal averaged over 10 potential scans[5].

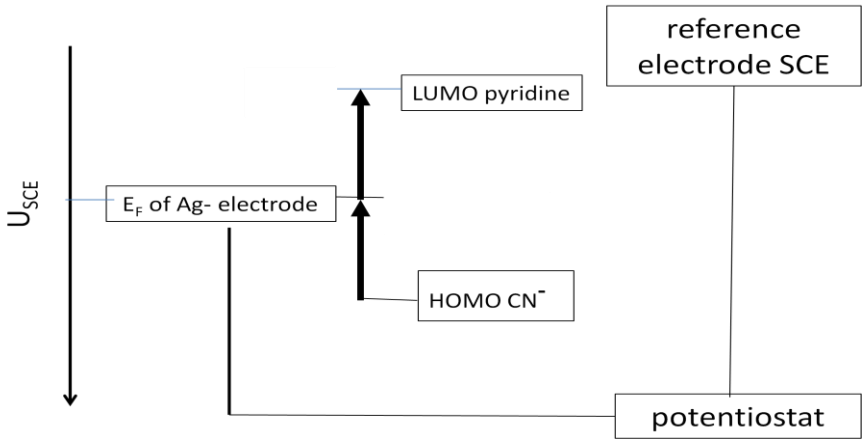

Figure 2) Controlling the Fermi level E_F of the silver electrode with respect to the standard calomel electrode (SCE) by a potentiostat. HOMO = Highest occupied molecular orbital, LUMO = Lowest unoccupied orbital. Electron transfer energies from the Fermi-level E_F to the LUMO of pyridine and from the HOMO =Highest occupied of cyanate CN^- to E_F (given by thick arrows) vary according to the potential of the silver electrode U_{SCE} (left scale)

Figure 2 shows how the Fermi level of the Ag electrode is shifting according to the setting of the potentiostat, thus changing the charge transfer (CT) energies. If E_F(Ag) is moving upwards, the electron transfer energy from E_F to the LUMO of pyridine decreases, the electron transfer from CN^- to E_F increases. If the Laser photon energy equals the CT energy, the Raman scattering intensity as function of the electrode potential E will reach a maximum, as first measured by Jeanmaire and VanDuyne[5] with only one Laser wavelength at 514.5nm. (Figure 1).

The dependence of the Raman intensity of the different vibration modes of adsorbed pyridine on an activated silver electrode in 0.M KCl, 0.05M pyridine electrolyte as function of the electrode potential[9] is displayed in figure 3.

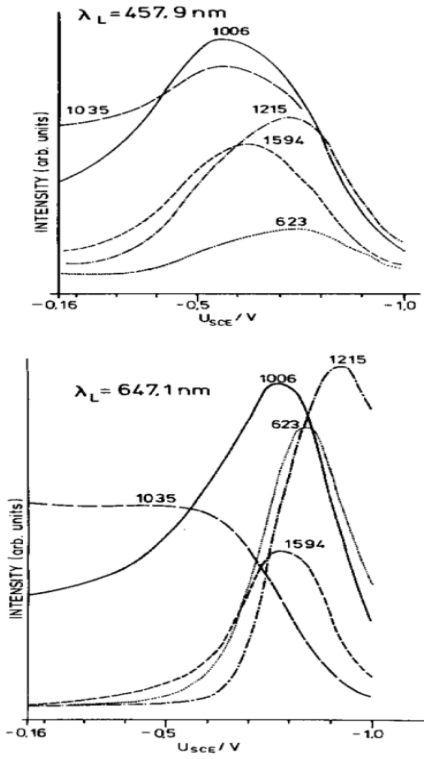

Figure 3) Intensity of adsorbed pyridine vibrational bands at about 623 cm^{-1}, 1006 cm^{-1}, 1035 cm^{-1} 1215 cm^{-1} and 1594 cm^{-1} versus potential of the polycrystalline activated silver electrodes measured with respect to a saturated calomel electrode (SCE). Laser wavelength 457.9 nm and 647.1 nm[9].

Figure 3 shows the expected shifts for pyridine. It is not known why the 1033cm^{-1} mode behaves differently than the other 4 modes. This has also been observed by Otero and co-workers[10].

The shifts of different vibrational modes are slightly different (see fig. 4). The peak positions of the relative intensities using 5 laser wavelengths between 457,9nm and 647.1 nm from Ar^+ and Kr $^+$Lasers are shown in figure 4.

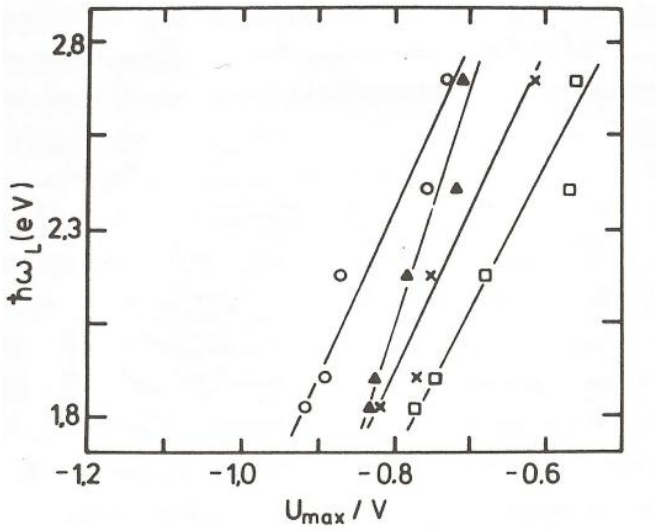

Figure 4) Electrode potentials $U_{max}(V_{SCE})$ at maximal intensity in fig. 3 left as function of the 5 Laser photon energies $\hbar(\omega_L)$, for pyridine vibrations at about 1215 cm^{-1} (open circles), 623 (black triangles), 1594 (crosses) and 1006 cm^{-1} (open rectangles). The electrolyte is 0.1M KCl, 0.05M pyridine[11]

The result of Jeanmaire and VanDuyne in Fig. 1[5] using only one Ar^+ Laser wavelength = 514.5 nm agree very well with the results in Fig. 4[9]

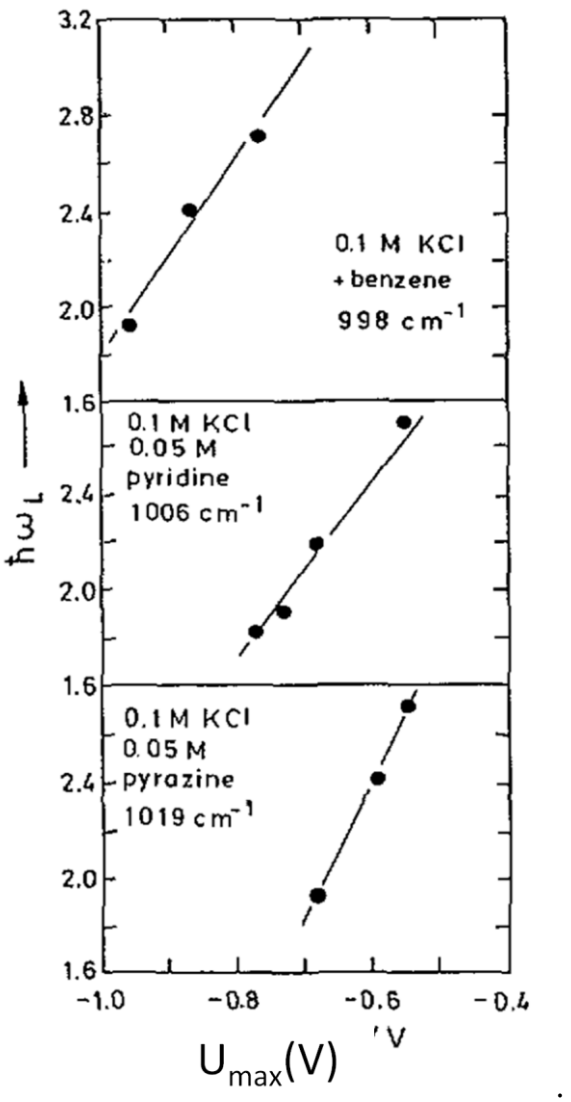

Figure 5) Full circles indicate the electrode potential P $_{max}$ (SCE) of maximal Raman intensity of the breathing modes of benzene, pyridine and pyrazine adsorbed at roughened silver electrodes in 0.1M KCl electrolyte versus laser photon energy $\hbar\omega_L$.

The results in figures 4 and 5 indicate that the maxima in figure 3 correspond to the electronic transition from the Fermi level of silver to the empty π^* level of pyridine. Also, the expected inverse shift for adsorbed CN^- has been ob served, see figures 6 and 7.

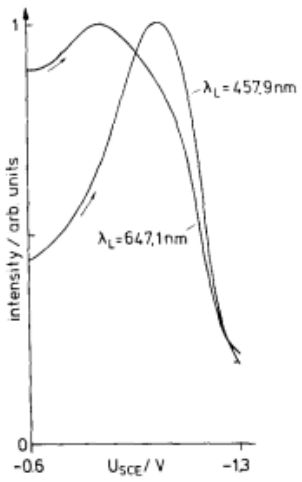

Figure 6) Intensity of the CN^- stretch vibration as a function of potential U_{SCE} for cathodic sweeps with 50 mV/s for 2 exciting Laser lines with Laser wavelengths λ_{Laser} as function of the potential of the silver electrode U_{sce}. The direction of the sweeps is indicated[11].

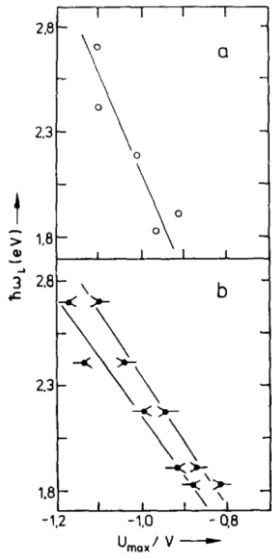

Figure 7) Silver electrode potential U_{max}, of maximal CN^- stretch SERS intensity versus excitation energy $\hbar\omega_L$(eV): (a) for cathodic sweep with 50 mV/s; (b) for cathodic (<) and anodic (>) sweeps with 500 mV/s [11].

Similar results for SCN^- on silver electrodes have been obtained by Furtak et al [8].

It is surprising that the gradients $\partial\hbar\omega_L / \partial U_{max}$ are bigger than 1. This has been explained in detail by Otero and co-workers [10]. They envision small Ag clusters at the roughened silver electrode as "SERS active sites" where the aromatic molecules are absorbed.

Also for the case of CN^- on Ag clusters, the measured gradient $\frac{\partial\hbar\omega_L}{\partial U_{max}} < -1$ yields $\left[\frac{\partial\hbar\omega_L}{\partial U_{max}}\right] > 1$.

For a given electrode potential, the π^* level of pyrazine is closer to the Fermi level, compared to π^* level of pyridine, see figure 5. This is corroborated by the results of inverse photoemission described below. Given all the results at silver electrodes, the electron transfer mechanism is confirmed. The necessary "roughening" or "activation" of the silver electrodes by oxidation-reduction cycles needs an explanation. It delivers electromagnetic enhancement of the Raman spectrum at the electrode surface and creates Ag-molecule complexes with resonances by transient internal electron transfer, as compiled in figure 26 of ref. [12]. SERS of adsorbates on roughened electrodes is quenched by exposure to air as observed by J. Billman and A. Otto (unpublished). The quenching of SERS at cold-deposited Ag films by a small exposure to O_2 (smaller than needed for complete coverage) has been observed[14]. The quenching by oxygen is cancelled, when the oxygen reacts formiate to formate[15]. Also the optical absorption by transition of an electron from Ag atoms to ethylene molecules observed in matrix isolation is quenched by O_2 [16]. In conclusion, quenching of SERS by oxygen is caused by

the oxidation of silver - adsorbate complexes.

In order to control the adsorption and desorption of simple molecules (for instance CO, benzine, pyridine, pyrazine) on clean noble metal surfaces, experiments must be performed in ultrahigh vacuum (UHV)-vessels at low temperatures. Samples are cleaned by sputtering and annealing at high temperatures, measuring of the orientation of the single crystal surfaces by low energy electron diffraction (LEED) to control the adsorbate coverage by needle valves, use of cryostats, mass spectrometers for thermo-desorption experiments (TDS), electron energy spectrometers for electron energy loss spectroscopy (EELS), ultraviolet photon emission (UPS) and Auger spectroscopy, and detectors for inverse photoemission. These surface science methods are not needed and no more considered in applied SERS-research, based on high electro-magnetic resonances in tailored plasmonic structures in air.

Measurement of the position of the LUMO with respect to the Fermi level.

In this and the following chapters, the adsorbates are physisorbed. They desorb at low temperatures, pyridine between 159-172K[17], and CO on smooth room temperature deposited silver films at 41K[18].

The energy difference between the LUMO of the adsorbate and the Fermi energy E_F of silver is measured by inverse photon emission. In this spectroscopy, electrons are incident on the silver surface covered by the adsorbate and photons are emitted. The electrons can only settle into energy states of silver above E_F and into unoccupied states of the adsorbates on the metal. From inverse photon emission follows, that the LUMO of pyridine is about 3 eV above the Fermi level, see figure 8. For pyrazine, the LUMO is about 2.5 eV above E_F [19].

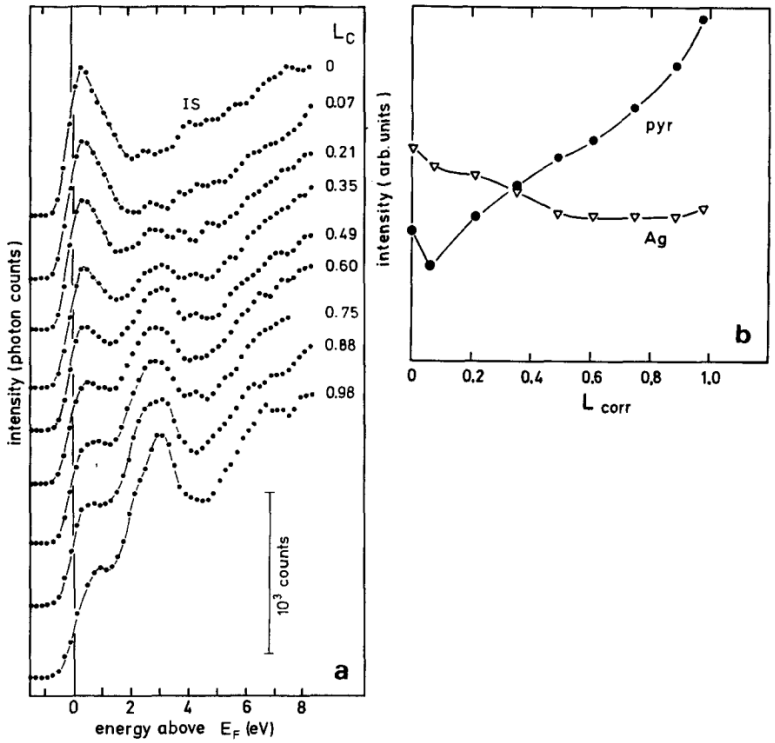

Figure 8(a) Inverse photon emission spectra (incident photon energy = 9.7 eV) for normal electron incidence on Ag (111) continuously exposed to pyridine (0 to 0.98 $L_{corrected}$) [20]. The

image state of Ag(111)[19] is denoted by IS, the pyridine peak is at about 3 eV energy above E_F. **(b)** Peak intensity of the peak or shoulder near 1 eV above E_F, labeled Ag and near 3 eV, labeled pyr, versus exposure to pyridine, given in Langmuir L corrected by the sensitivity of the mass spectrometer (L_{Corr})

In figure 9, the inverse photon emission spectra of pyridine and pyrazine on Ag(111) are compared.

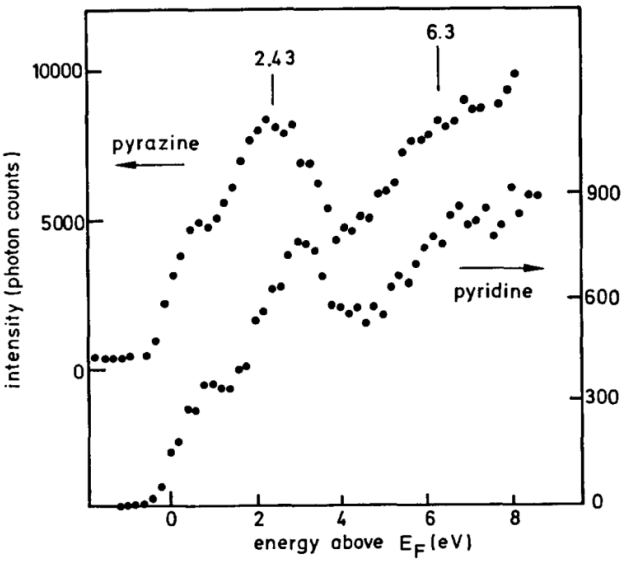

Figure 9) Inverse Photon emission of pyridine C_5NH_5 and pyrazine $C_4N_2H_4$ adsorbed on Ag(111), exposure 0.98 L_C [19].

From figure 9 follows that the electron transfer energies from E_F to the LUMO's of pyridine and pyrazine are in the range of the photon energies used in the electrochemical experiments in chapter 1, (20000 cm^{-1} correspond to 2.396eV). Therefore, the inverse photon spectroscopy results support the results of electron transfer reactions at silver electrodes in Fig. 5.

The first layer effect

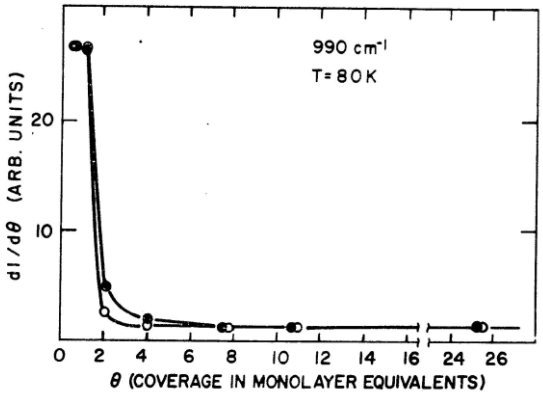

Figure 10) Incremental intensity of the pyridine breathing vibration at 990cm^{-1} as function of the adsorbed monolayers[21].

Sanda et al [21] measured the Raman signal as a function of the number of the adsorbed pyridine layers on a specially prepared silver (111) sample with a controlled surface modulation of 1000nm length and 100nm amplitude, to profit from the extra EM enhancement in surface plasmon polariton resonance. 90 % of this surface are (111) oriented. A large mode selective enhancement was measured, about 10^4 of the Raman signal from the first monolayer and about 10^2 for multilayers. The first layer frequency of the breathing mode of pyridine is 990 cm^{-1} (see Figure 10.) This Raman wavenumber indicates clearly that pyridine adsorbed on the (111) surface is observed, in agreement with Campion's results on pyridine adsorbed on Ag(111) [22]. The 990 cm^{-1} was also observed for pyridine adsorbed on smooth silver films with (111) orientation, deposited at room temperature (figure 1 in [23]). On the stepped Ag(540) surface, Campion and Mullins[24] detected the breathing mode at

about 1000cm$^{-1.}$ Both on roughened Ag electrodes[5], (see Figure 1), on cold deposited Ag films[25] and on silver films on nanospheres (AGFON)[26] the breathing mode is at 1006cm^{-1}. After "regeneration" of an AGFON sample, the mode 992cm^{-1} reappeared[17]. The breathing mode wavenumber of condensed pyridine is 996cm^{-1} [27].

It follows, that the Raman signal at 990 cm^{-1} measured by Sanda et al[21] originates from a monolayer of pyridine adsorbed on Ag (111) .

The first layer effect was also observed on silver island films produced in situ by thermal evaporation on a sapphire substrate at room temperature. After cooling the island film to 30K it was exposed to various sequences of hydrogenated and deuterated pyridine[28]. The Raman intensity was measured in the range of the breathing modes of the two isotopic species. (Figure 11).

The Raman spectra in figure 11 were taken with a laser power of about 90mW in the frequency range of the pyridine ring breathing mode. The bands 1,2,3 belong to C_5NH_5, the bands 4,5,7 belong to C_6ND_5. Left side, spectrum a): First exposure at to 4L C_5NH_5 (about one monolayer), further exposure to 16L C_5ND_5 (about 4 monolayers), directly afterwards the sample was heated from 30K to b) 92K, c) 140K, d)157K. Right side (second experiment): e) First exposure at 30K to 4L of C_5ND_5 (about 1 monolayer) followed by f) 16L of C_5NH_5 (about 4 monolayers) at 30K ,g) directly afterwards heated to 140K and h) 157K [28]. At temperatures above 30K, the two isotopic species start intermixing. These results demonstrate, that only the isotopic species which forms the first monolayer on the island film contribute to SERS. The second layer yields no signal. The long range EM enhancement given by the silver islands is necessary to boost this Raman intensity. However this EM enhancement is comparatively long range[29], extending beyond the first layers of pyridine.

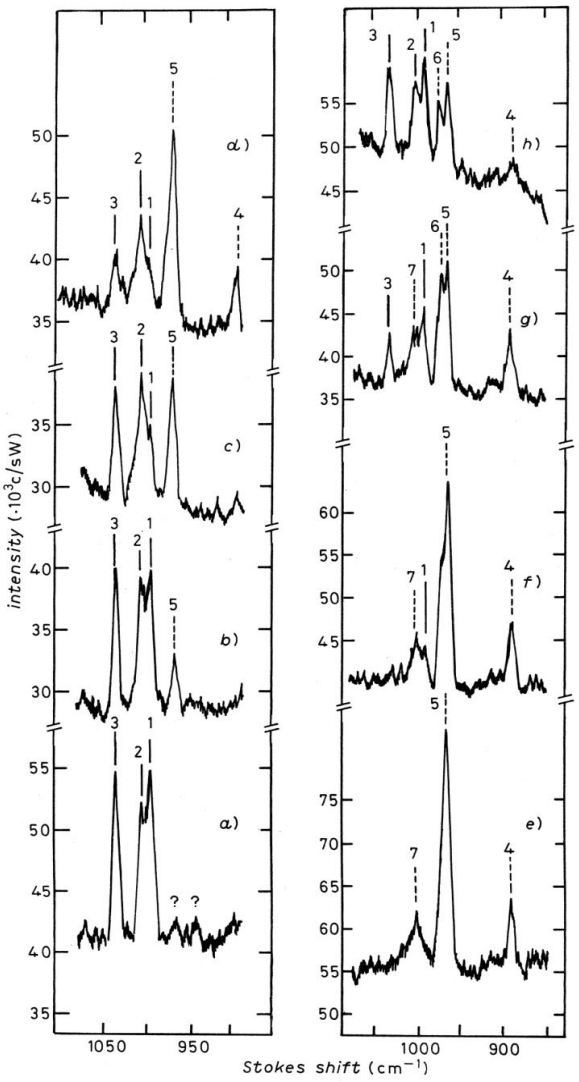

Figure 11) SERS of C_5NH_5 and C_5ND_5 on a silver island film (deposition rate 0.1-0.2 nm/s on a cooled sapphire substrate (temperature 30K), with average film thickness about 6.3nm., bands 1,2,3 belong to C_5NH_5 , bands 4,5,7 belong to C_5ND_5 .

The first layer effect and long range enhancement were also measured by introducing spacer layers [30], see figure 12.

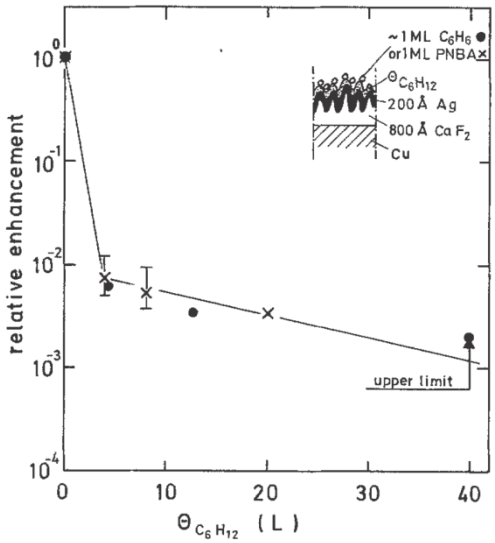

Figure 12) Relative enhancements of Raman intensities for monolayers of benzene C_6H_6 (points) and para-nitrobenzoic acid PNBA (crosses) versus thickness of the spacer layer of cyclohexane C_6H_{12}, see inset [30]. Temperature T=30K.

The electromagnetic enhancement was achieved by evaporating CaF_2 of 80nm thickness on a cooled flat Cu substrate. The roughness of the CaF_2 layer increases with its thickness[31]. CaF_2 films of 80nm thickness have a rms roughness of 4nm and an autocorrelation length of 20nm[31]. The evaporated silver films on top of the CaF_2 film have a thickness of 20nm. The thickness of the cyclohexane (C_6H_{12}) spacer layer is given in units of the exposure Θ_{C6H12} (see the inset of Figure 12). The relative Raman intensities of monolayers of benzene at 990cm^{-1} and of nitrobenzoic acid (PNBA) at 1598cm^{-1} depend on the precoverage of C_6H_{12}. The strong enhancement at $\Theta_{C6H12} = 0$ is assigned to the product of the first layer enhancement and the long range EM enhancement. The long range enhancement at $\Theta_{C6H12} > 4$ is assigned to pure EM enhancement. It follows that the first layer enhancement is about 100.[30] A diffusion of C_6H_6 or PNBA through the $C_{12}H_{12}$ spacer layer can be excluded, because in this case the enhancement would not depend on the thickness of the spacer layer.

Electron transfer excitations observed by EELS.

Electron transfer excitations have been observed by electron energy loss spectroscopy with low energy electrons. From the loss spectra of internal molecular vibrations , Demuth and Avouis concluded, that pyrazine adsorbs flat on the Ag(111) surface[32], whereas pyridine is inclined on the surface, as also found by near edge x-ray absorption fine structure (NEXAFS)[33].

Avouris and Demuth[32] detected an electron transfer excitation from silver(111) exposed to pyrazine and pyridine, see figure 13.

In figure 13 left, the energy loss spectrum of clean Ag(111) surface does not show a structure at about 2eV. After an exposure of 1Langmuir of pyrazine (corresponding to one monolayer) there appears a weak structure at the energy loss energy 2eV. This structure is lost at an exposure of 4.5L, but reappears after heating the sample to 220K as a broad feature peaked at 2.3 eV, which is assigned to an electron transfer excitation from silver(111) to adsorbed pyrazine.. This energy loss is assigned to an electron transfer from silver(111) to physisorbed pyrazine in the first monolayer. A similar structure at about 2.3eV has been observed for pyridine on Ag(111) in off specular condition (fig. 13 right). These losses have been assigned to electron transfer by Avouris et al[32].

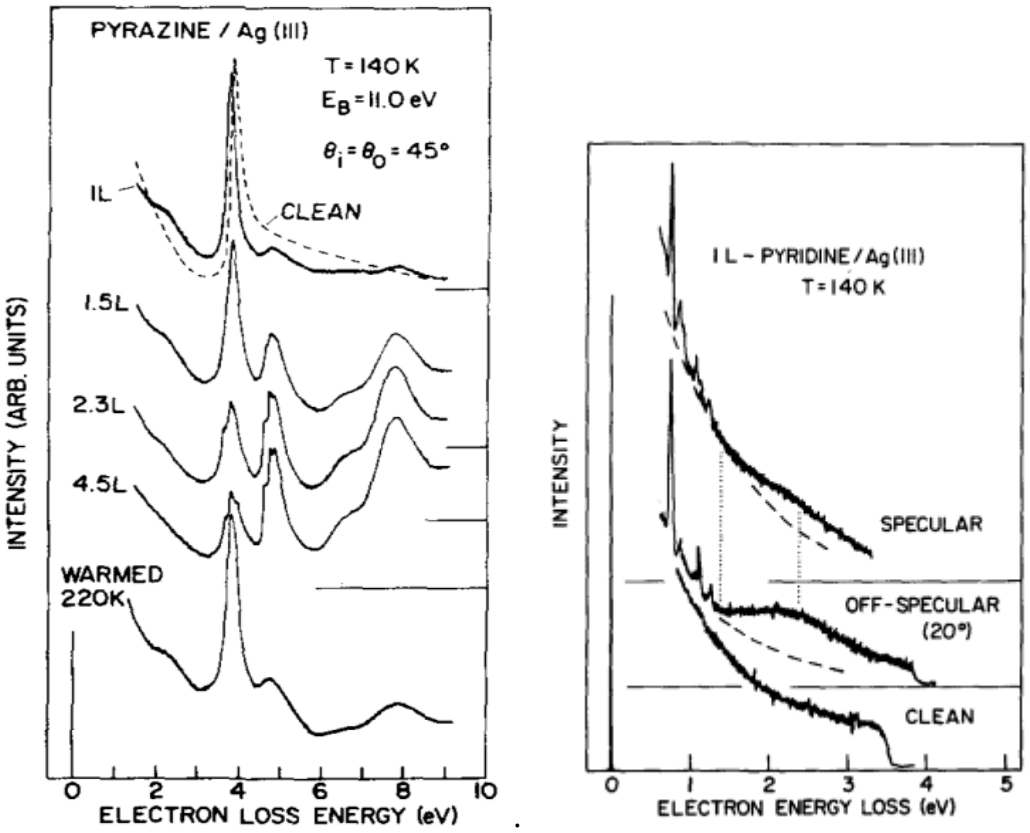

Figure 13) Left: Electronic-energy-loss spectra for clean Ag(111) and as a function of pyrazine exposure, with scattering conditions $\Theta_{in} = \Theta_{out} = 45^0$ and electron beam energy E_B=11eV with full width at half maximum of 30 mV. [32] Right: Energy loss spectra of pyridine on Ag(111) in specular and off-specular condition as function of scattering angle and E_B =3.9eV [32]

Electron transfer reactions causing surface resistance.

A related effect to the first layer SERS is also observed in the increase of the resistance of thin silver films. See figures 14 and 15.

Like in the first layer effect SERS, only the first adsorbed layer contributes to the surface resistance. This is explained with the help of fig 14. At the smooth surface of a thin Ag film electrons are specularly reflected. When a molecular monolayer is adsorbed, for instance ethene (C_2H_4), an electron may be transferred to the LUMO (lowest unoccupied orbital) and scattered in various directions. The empty reflected state is the hole. The creation of electron hole pairs is the cause of the surface resistance.

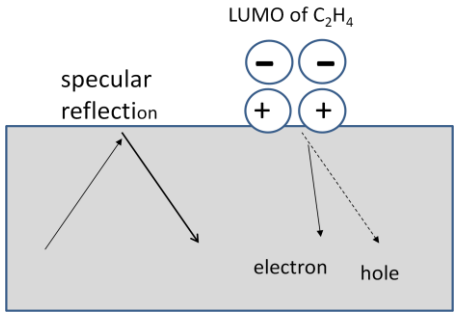

Figure 14 Scheme of the creation of electron hole pairs by transient electron transfer

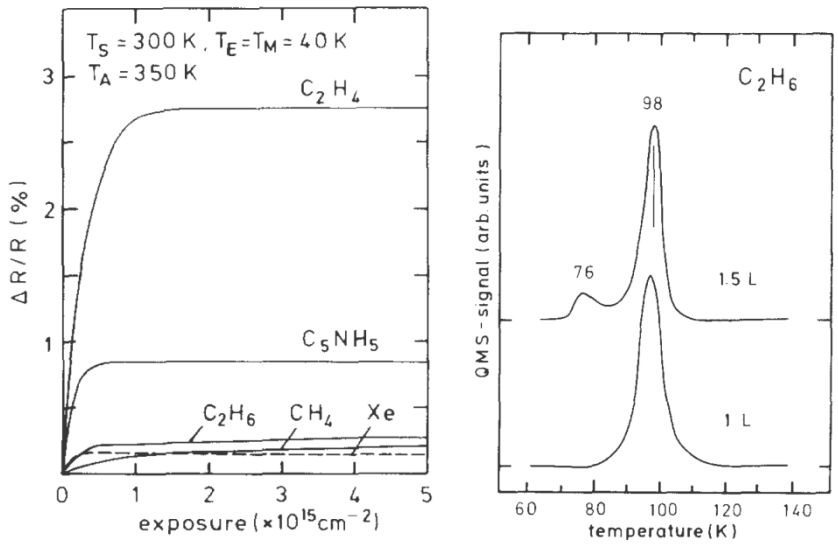

Figure 15 (left): Resistance R and resistance variation ΔR of silver films, deposited at 300K in ultrahigh vacuum (UHV), annealed at 350K and cooled to 40K, and measured at 40K during exposure with CH_4 , C_2H_4, C_2H_6, C_5NH_5 and Xe. The resistance R at 40K before exposure was 0.35, 0.32, 0.31, 0.30 and 0.77 Ohm respectively[34].

Figure 15 (right): Thermo desorption spectra of C_2H_6 adsorbed on smooth silver film exposed to 1 and 1.5 L of C_2H_6, with heating rate of about $1.5Ks^{-1}$, measured with a quadrupole mass spectrometer (QMS)[34.34].

The annealing of the silver films at 350K to guarantees smooth silver films of (111) orientation. The exposure to 10^{15} molecules /cm^2) corresponds approximately to the formation of one monolayer at sticking coefficient 1. In any case, multilayers desorb at higher temperatures than the first layer. An example is shown in figure 15 right for C_2H_6. (Fig. 15 (right)). The first monolayer desorbs at 100K, the additional adsorbed layers desorb at 76K. For the 5 kinds of adsorbates the relative resistance change $\frac{\Delta R}{R}$ becomes constant above an exposure of about $1x10^{15}$ molecules per cm^2. This corresponds to the formation of the first monolayer. The growth of further layers does not change the resistance, as expected. However, the saturation values of R depend strongly on the adsorbate. ΔR is the surface resistance.

The surface resistance ΔR can be explained by transient electron transfer from the silver surface to the first layer of adsorbates. The noble gas Xe has a filled electron shell and does not accept electrons. Methane CH_4 and ethane C_2H_6 have no empty π^* states, only σ^* states at higher energy and hence there is little transient electron transfer from the Fermi level E_F of silver to the σ^* states. However, the pyridine π^* state of pyridine adsorbed on the Ag(111) surface is only 3 eV above the Fermi energy E_F , as measured by inverse electron spectroscopy [20]. For ethene C_2H_4, the π^* level is probably closer to E_F and hence $\frac{\Delta R}{R}$ is larger in comparison to pyridine.

Summary

The Raman scattering intensity of the vibrations of pyridine and CN^- adsorbed on roughened silver electrodes depend on the electrochemical potential of the electrode and on the laser photon energy. The observed resonances are explained by electron transfer from the Fermi level of the silver electrode to the lowest unoccupied orbital (LUMO) of adsorbed pyridine and from the highest occupied orbital (HOMO) of adsorbed CN^- to the Fermi level of the silver electrode. The positions of the lowest unoccupied orbitals (LUMO) of pyridine and pyrazine adsorbed on Ag(111) were measured by inverse photo-electron emission spectroscopy. These results support the charge transfer model. An extra enhancement of about 100 for the first adsorbed layer on Ag (111) in ultra high vacuum was detected by Sanda et al [21] by enhancing the EM field. A first layer enhancement was also observed on silver island films and on Ag films contouring a CaF film [28]. In this case, one observes both the first layer enhancement of about 100 and the long range EM enhancement. The electron transfer energies of 2-3eV have been measured by low energy loss spectroscopy for pyridine on Ag(111)[32], supporting the charge transfer model. This model explains also the surface resistance induced by various adsorbates.

Literature

1. Moskovits, M. Surface roughness and the enhanced intensity of Raman scattering by molecules adsorbed on metals *J.Chem.Phys.* **1978** *69*.

2. Creighton, J. A. Surface enhanced Raman electromagnetic enhancement factors for molecules at the surface of small isolated metal spheres, the determination od adsorbbate orientation from SERS relative intensities *Surface Science* **1983,** *124*.

3. Burstein, E.; Chen, Y. J.; Chen, C. Y.; Lundquist, S.; Tosatti, E. "Giant"Raman scattering by adsorbed molecules on metal surfaces. *Solid State Communications* **1979,** *29*.

4. Fleischman, M.; Hendra, P. J.; McQillan, A. J. Raman Spectra from Electrode Surfaces *J.C.S.Chem.Comm.* **1973,** *26*.

5. Jeanmaire, D. L.; VanDuyne, R. P. Surface Raman spectro-electrochemistry, part 1:heterocyclic aromatic and aliphatic amines adsorbed on the anodiced silver electrode. *J.Analytic Electrochemistry* **1977,** *84*.

6. Albrecht, M. G.; Creighton, J. A. Anomalously intense Raman spectra of pyridine at a silver electrode *J.American Chemical Society* **1977,** *99*.

7. Chang, R. K.; Furtak, T. E. *Surface enhanced Raman scattering* New York, 1982.

8. Furtak, D. E.; Trott, G.; Loo, B. Light sattering from the metal/solution interface ,chemial origins. *Surface Science* **1980,** *101*.

9. Billmann, J.; Otto, A. Electronic Surface-State Contribution to Surface Enhanced Raman-Scattering. *Solid State Communications* **1982,** *44*.

10. Roman-Perez, J.; Ruano, C.; Centeno, S. P.; López-Tocón, I.; Arenas, J. F.; Juan Soto, J.; Otero, J. C. Huge Energy Gain in Metal-to-Molecule Charge Transfer Processes: A Combined Effect of an Electrical Capacitive Enhancement in Nanometer-Size Hot Spots and the Electronic Structure of the Surface Complex. *J.Physical Chemistry C* **2014,** *118*.

11. Billman, J.; Otto.A. Charge transfer beween adsorbed cyanide and silver probed by SERS. *Surface Science* **1984,** *138*.

12. Otto, A.; Mrozek, I.; Grabhorn, H.; Akemann, W. Surface-Enhanced Raman-Scattering. *Journal of Physics-Condensed Matter* **1992,** *4* (5), 1143-1212.

13. Otto, A. Surface enhanced Raman scattering. *J.Raman Spectroscopy* **1991,** *22*.

14. Pettenkofer, C.; Eickmans, J.; Ertürk, Ü.; Otto, A. On the nature of "SERS active sites". *Surf.Sci.* **1985,** *151*.

15. Pohl, M.; Pieck, M.; Hanewinkel, C.; Otto, A. A Raman Study of Formic Acid and Surface Formate Adsorbed on Cold-deposited Copper Films. *J.Raman Spectroscopy* **1996,** *2*.

16. McIntosh, D. F.; Ozin, G. A.; Messmer, R. P. *Inorg.Chemistry* **1880,** *19.*

17. Litorja, M.; Haynes, C. L.; Haes, A. J.; Jensen, T. R.; VanDuyne, R. P. Surface-Enhanced Raman Scattering Detected Temperature Programmed Desorption: Optical Properties, Nanostructure, and Stability of Silver Film over SiO2 nanoshere surfaces. *J. Phys. Chem. B* **2001,** *105*.

18. Pettenkofer, C.; Mrozek, I.; Borneman, T.; Otto, A. On the contributionof classical electromagnetic field enhancement to Raman scattering from adsorbateson coldly

deposited silver films. *Surface Science* **1978,** *188*.

19. Otto, A.; Reihl, B. EELS, Inverse and Direct Photoemission of Pyrazine on Ag(111). *Surface Science* **1986,** *178*.

20. Otto, A.; Frank, K. H.; Reihl, B. Inverse Photoemission of Pyridine on Silver(111). *Surface Science* **1985,** *163*.

21. Sanda, P. N.; Warlaumont, J. M.; Demuth, J. E.; Tsang, J. C.; Christmann, K.; Bradley, J. A. Surface-enhanced Raman scattering from pyridine on Ag(111). *Phys.Rev.Lett.* **1980**.

22. Campion, A. Spectroscopy without enhancement: pyridine on Ag(111). *Journal of Electron Spectroscopy and Related Phenomena* **1983,** *29*.

23. Ertürk, U.; Otto, A. Raman Enhancement for Pyridine on Smooth Silver by Submonolayer Deposition of Silver. *Europhysics Letters* **1988,** *6*.

24. Campion, A.; Mullins, D. R. Unenhanced Raman scattering from pyridine adsorbed on stepped and kinked silver surfaces under ultrahigh vacuum. *Surface Science* **1985,** *158*.

25. Pockrand, I.; Otto, A. Coverage Dependence of Raman-Scattering from Pyridine Adsorbed to Silver-Vacuum Interfaces. *Solid State Communications* **1980,** *35* (11), 861-865.

26. Dick, L. A.; McFarland, A. D.; Haynes, C. L.; VanDuyne, R. P. *Metal Film over Nanosphere (MFON) Electrodes for Surface-Enhanced Raman Spectroscopy (SERS): Improvements in Surface Nanostructure Stability and Suppression of Irreversible Loss. *J. Phys. Chem. B* **2002,** *106*.

27. Grabhorn, H. Der Einfluß atomarer Rauhigkeit auf die oberflächenverstärkte Ramanstreung von Adsorbaten an Silberoberflächen. Heinrich-Heine-Universität, Düsseldorf, 1991.

28. Mrozek, I.; Otto, A. Long-Range and Short-Range Effects in SERS from Silver. *Europhysics Letters* **1990,** *11*, 243.

29. Kovacs, G. J.; Loutfy, R. O.; Vincett, P. S.; Jennings, C.; Aroca, R. Distance Dependence of SERS Enhancement Factor from Langmuir-Blodgett Monolayers on Metal Island Films:Evidence for the Electromagnetic Mechanism. *Langmuir* **1986,** *2*.

30. Mrozek, I.; Otto, A. SERS - a Long-Range Effect? *Applied Physics a-Materials Science & Processing* **1989,** *49*, 389.

31. Rasigni, G.; Varnier, F.; Palmari, J. P.; Mayani, N.; Rasigni, M.; Llebaria, A. Study of surface roughness for thin films of CaF_2 deposited on glass substrates. *Optics communications* **1983,** *46*.

32. Avouris, P.; Demuth, J. E. Electronic excitations of benzene, pyridine, and pyrazlne adsorbed on Ag(111) *J. Chem. Phys.* **1981,** *76*.

33. Bader, M.; Haase, J.; Frank, K.-H.; Puschmann, A.; Otto, A. Orientational Phase Transition in the System Pyridine/Ag(111): A Near-Edge X-Ray-Absorption Fine-Structure Study. *Phys.Rev.Lett.* **1968,** *56*.

34. Holzapfel, C.; Akemann, W.; Schumacher, D.; Otto, A. Variations of Dc-Resistance and SERS Intensity During Exposure of Cold-Deposited Silver Films. *Surface Science* **1990,** *227* (1-2), 123-128.

